Multi-Layered Proximity Probe-Fed E-Shaped Patch Antenna Array for Terahertz Imaging System

Ian Huang*, Ling-Yun Kung*, Shih-Yuan Chen†,
*Graduate Institute of Communication Engineering, National Taiwan University, Taipei 106, Taiwan
†Department of Electrical Engineering, National Taiwan University, Taipei 106, Taiwan
f06942135@ntu.edu.tw, kunglingyun85@gmail.com, shihyuan@ntu.edu.tw

***Abstract*—This work presents a multi-layered proximity coupled meandering-probe-fed E-shaped patch antenna array for terahertz imaging system with a center frequency at 150 GHz. The E-shaped patch antenna is proximity coupled using a meandering-probe feed. A test kit was designed, fabricated, and measured to verify the design and resonance of the E-shape patch antenna. An antenna feeding structure was also designed, with a 2.52 dBi total broadside realized gain of the antenna and feeding structure combined. A 4×4 subarray provided a 30% impedance bandwidth and an 80% radiation efficiency. A decoupling design for the antenna array was also proposed.**

***Index Terms*—terahertz wave imaging, IC substrate, E-shaped patch antennas, meandering-probe.**

I. Introduction

Terahertz radiation is located between millimeter waves and infrared light waves on the frequency spectrum. This frequency band had previously been widely utilized partly due to the difficulties and scarcity of generating radiative sources. Recent advancements in terahertz devices have improved their applications, including imaging, security scanning, and terahertz communications. When looking at terahertz imaging, its antennas need to have characteristics of wide operating bandwidth, high gain, and good radiation efficiency. Previously proposed antennas used in terahertz imaging include photoconductive antennas [1], leaky-wave antennas [2], lens antennas [3], microstrip antennas [4], and on-chip antennas [5] and [6]. When integrating with the entire imaging system, oftentimes the antenna array design will need to be compatible with the system setup and packaging process. This work focuses on an antenna array design implemented on a multi-layered printed circuit board (PCB). A proximity-coupled meandering probe is used to excite the E-shaped patch antennas, a feeding structure was designed to be compatible with the packaging process, and a decoupling structure was designed for the array.

II. Antenna Array Design

A terahertz imaging system to physically and electrically reconstruct an unknown object is proposed. The operation principle of this imaging system is to use the magnitude and phases of the signal that is reflected off the unknown object to find out the distance between the imaging system and the target. By applying these obtained data with the Huygens-Fresnel Principle, the object's material properties and shape can then be obtained and reconstructed. This proposed system will operate at a center frequency of 150 GHz, with one transmitting channel and 256 receiving channels. The system will be introduced below in more detail, with a focus on the system's antenna array and antenna feeding network.

A. Terahertz Imaging System

A 12.5 GHz Continuous-Wave (CW) signal source is input into the system for both the transmitter and receiver and goes through a ×12 frequency multiplier to become a 150 GHz signal. For the transmitter, the signal is output using a horn antenna due to its high gain and wide bandwidth.

The receiver consists of a motherboard, integrated circuits (ICs), and a daughterboard. The daughterboard connects the antenna array and ICs to the rest of the system. From the signal source, the receiver also receives a reference 150 GHz signal that has passed through a ×12 frequency multiplier to then go into a WR-06 waveguide, then fed into a substrate-integrated waveguide (SIW) within the motherboard.

The motherboard consists of a four-layered PCB, which sends the signal through a quasi-coaxial cable to the daughterboard to act as reference signals. The daughterboard shown in Fig. 1 is made of the top build-up, the bottom build-up, and the core. For the top and bottom sections, each metal layer is separated by 40-μm thick BT (Bismaleimide-Triazine) resin substrate (GHPL-970LF). The core comprises of a 100-μm thick substrate of HL-970LF, with similar material properties to the BT layers. Layers 1-4 on the daughterboard are used for antenna design, while metal layers 5-10 are used for the antenna feeding structure, the power delivery network, and the dc control lines.

B. E-Shaped Patch Antenna

To integrate with the system, patch antennas are chosen due to their planar profile for integration with circuit components. However, patch antennas suffer from a low impedance bandwidth, so an E-shaped antenna is used to achieve a more wide-band characteristic [7]. A first resonant mode is caused by the current flow in the middle of the patch antenna; the pair of slits inserted at one of the radiation edges creates a longer path for a current path to flow along the edge of the slits, which creates a second resonant mode. Combining the two resonant modes in adjacent frequencies thus can create a wider bandwidth.

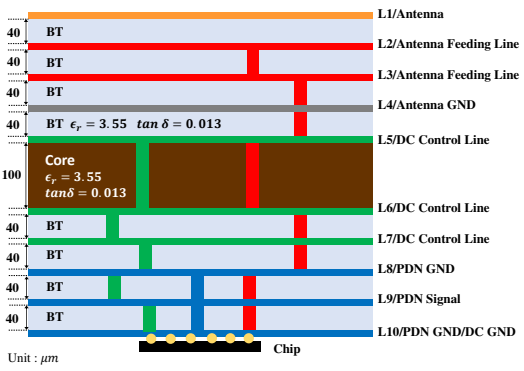

Fig. 1. Stackup of the daughterboard.

C. Feeding of E-Shaped Patch Antenna

The proposed feeding method for the E-shaped patch antenna uses proximity coupling through a meandering probe, which is based on an L-shaped probe. Other common methods are to use microstrip-line feed-in that has considerable spurious radiation leakage, coaxial probe feed-in that has large inductances when using thick substrates and also introduces significant manufacturing difficulties when considering system integration, and aperture coupling that has significant back radiation from the aperture slot. Proximity coupling was chosen due to its wide bandwidth characteristic, its low spurious radiation, and its compatibility with the system's multi-layer fabrication requirements.

In [8] and [9], an L-shaped probe-fed patch antenna with 36% impedance bandwidth is introduced. The horizontal section of the probe that is parallel to the patch antenna introduces a capacitance, which can also suppress some of the original inductance that the original straight probe would have. This series L-C resonance is connected in series to the patch antenna's R-L-C resonant element, and when the L-probe's L-C resonance is close to the TM_{01} mode of the patch antenna, this can allow for wideband operation. Previous demonstrations of an E-shaped patch antenna with an L-shaped probe-feed can be found at [10] and [11].

When considering the fabrication of this L-shaped probe feed, the vertical portion of the probe will need to be made of vias. Due to fabrication limitations, only a maximum of two vias can be aligned vertically, so vias that need to pass through multiple layers will need to be offset. In the proposed system, the receiving antenna will be in layers 1-4 of the daughterboard, with the E-shaped patch on layer 1 and the antenna ground on layer 4. Layer 2 and 3 vias of the L-shaped probe feed can be aligned as shown in Fig. 2b, while a meandering offset design of the two layers can be seen in Figs. 2c and 2d. A parametric study compared an ideal probe feed, an L-probe, and a meandering probe. The results showed similar co-polarization levels for both E- and H-planes for all three, while the cross-polarization varied with frequency for all except the meandering probe. This is due to the distances between the vias of Layer 2 and 3 being approximately half-wavelength, causing the currents of the two vias to be opposite, which then suppresses the unwanted radiation from the vertical section of the probe that contributes to cross-polarization.

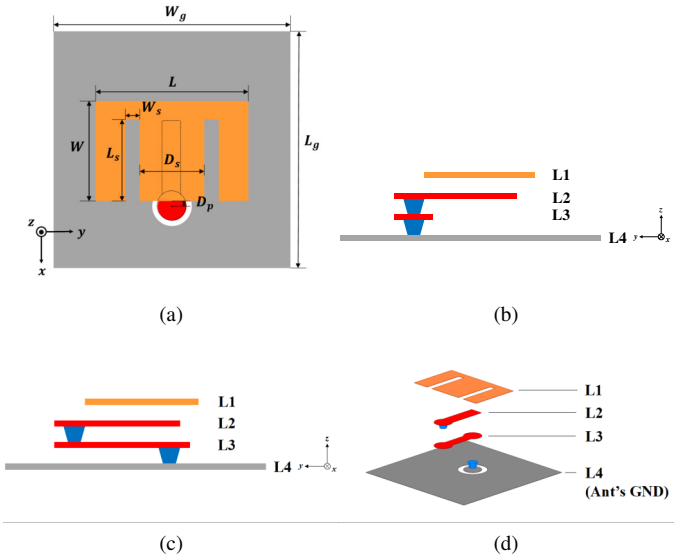

Fig. 2. (a) Top view of antenna fed by meandering-probe (W_g = 1 mm, L_g = 1 mm, L = 630 µm, W = 380 µm, L_s = 325 μm, W_s = 50 μm, D_s = 270 μm, D_p = 20 μm, W_p = 100 μm, L_p = 340 μm, L_c = 300 μm, W_c = 80 μm, D_{pad} = 135 μm, $D_{Antipad}$ = 215 μm); (b) side view of aligned L-Probe; (c) side view of meander probe; (d) 3-D perspective view of meander probe.

D. Antenna Feeding Structure

To feed the received signal from the antenna on Layer 1 to the circuits mounted at the bottom of the daughterboard on Layer 10, a feeding structure must be designed. When designing the feeding structure, the fabrication limitations previously mentioned, such as having a maximum of two vias vertically aligned and the limited space for design, cause the structure to be more complex. The final feeding structure is presented in Fig. 3.

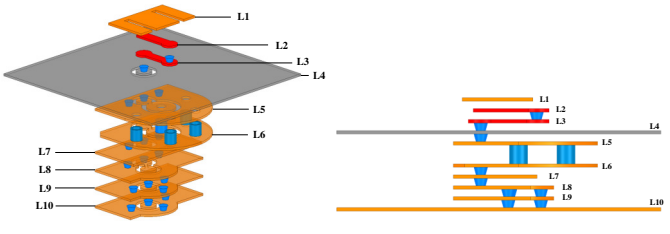

Fig. 3. (a) 3-D perspective view and (b) side view of feeding structure through layers 1-10.

E. E-Shaped Patch Antenna Array

The terahertz imaging system requires a 16×16 array, which is subdivided into 64 2×2 subarrays. Each of these 2×2 subarrays is connected to one 6-port IC using the feeding structure mentioned above. The spacing between elements is 1 mm, which is the half-wavelength in free space at 150

GHz. For a 2×2 subarray, there are three different kinds of orientations for the E-shaped patch antennas. When factoring the nearby elements around the subarray, the feed-in-inward orientation that is located inside the dotted box shown in Fig. 4 was chosen due to its symmetry along both the *x* and *y* axis.

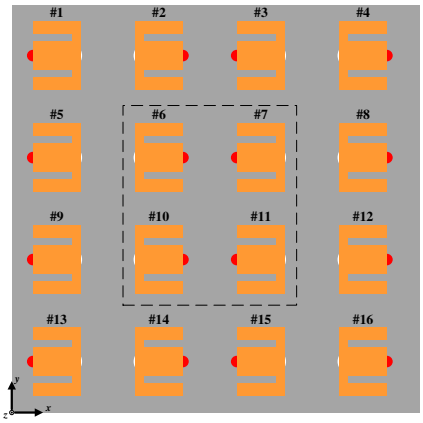

Fig. 4. 4×4 antenna array with the center 2×2 subarray orientated feed-in inward.

F. Decoupling Structure

To improve on the 16×16 antenna array, a decoupling structure was designed. Previous L-probe-fed arrays used metallic walls or via fences with slots in the ground plane [12] [13] [14] [15], but this isn't feasible due to manufacturing limitations. Other techniques include periodic structures, parasitic elements, neutralization line, and decoupling network. A goal for this structure is to have low complexity while still significantly reducing the mutual coupling in the operating band; therefore, a microstrip section for decoupling was the technique used. Therefore, two metallic strips of length R_{L1} were added in the E-plane of the analyzed 2×2 subarray, and one metallic strip of length R_{L4} was added in the H-plane of the subarray, with the configuration as shown in Fig. 5.

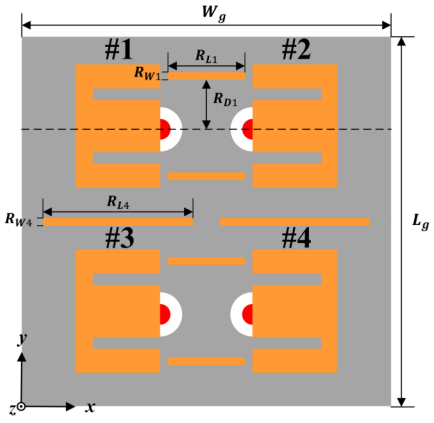

(a) a

Fig. 5. (a) The dimensions of the decoupling structure are $R_{L1} = 0.45\lambda_g$, $R_{w1} = 0.075\lambda_g$, $R_{L4} = 0.518\lambda_g$, $R_{w4} = 0.075\lambda_g$, $R_{D1} = 0.78\lambda_g$.

III. Simulation and Measurement Results

The circuits were analyzed using the Advanced Design System (ADS) software from Keysight, as well as the full-wave electromagnetic simulation software (High-Frequency Structure Simulator (HFSS) from Ansys.

A. E-shaped Patch Antenna with Meandering Probe-Feed

The S parameters, radiation efficiency, and broadside realized gain of the E-shaped patch antenna with an ideal probe-feed, an L-Probe feed, and a meandering-probe feed was simulated, as shown in Fig. 6. The ideal probe and L-probe has an impedance bandwidth of 23.1%, while the meandering-probe has an impedance bandwidth of 30.1%. All three have 88% radiation efficiency at the center frequency of 150 GHz. It can be seen that the meandering-probe has a higher realized broadside gain across all frequencies when compared to the L-probe, which confirms the choice of using meandering-probe to feed-in the patch antenna. The meandering-probe obtains a broadside realized gain of 6.02 dBi at 150 GHz.

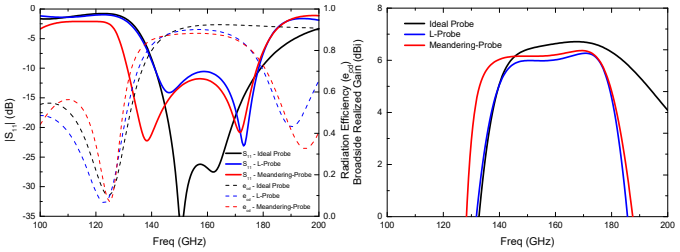

(a) (b)

Fig. 6. Simulated (a) reflection coefficient ($|S_{11}|$) and radiation efficiency (e_{cd}) and (b) broadside realized gain versus frequency using different feeding methods.

To verify the E-shaped patch antenna design, a test kit was designed and fabricated, as shown in Fig. 7. The on-wafer measurement was performed at Taiwan Semiconductor Research Institute (TSRI) using millimeter-wave extension modules (N5256AW08) with an output frequency from 140 GHz to 220 GHz. It was then connected to a waveguide probe, shown in Fig. 8a. The measured results of the test kit showed a similar resonance frequency as the designed E-shaped patch antenna resonance in Fig. 8b.

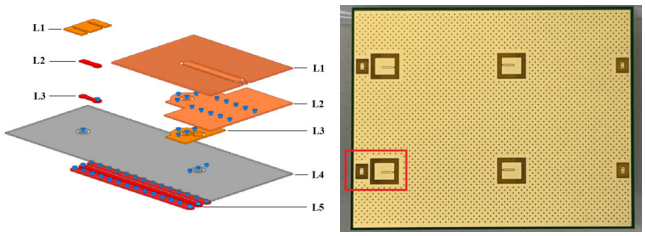

(a) (b)

Fig. 7. (a) 3-D view of the test kit, (b) Top view of the fabricated test kit (shown in the red box).

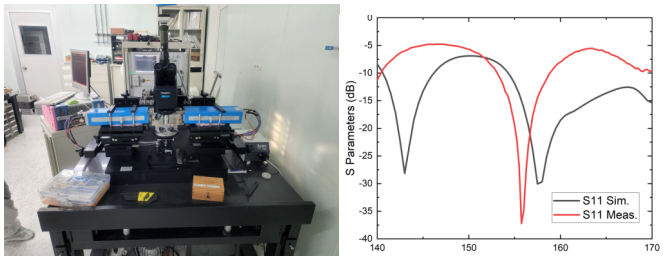

(a) (b)

Fig. 8. (a) Measurement setup of S-Parameters of E-shaped Patch Antenna, (b) S parameter simulation and measurement of test kit

B. Antenna Feeding Structure

The reflection coefficient and the radiation efficiency of Layers 4-10 are shown in Fig. 9. From simulation, Layers 4-10 has an insertion loss of 3.5 dB. When added to the broadside realized gain of the antenna in Layers 1-4 of 6.02 dB, the resulting 2.52 dBi is close to the 2.8 dBi value obtained when simulating the combined Layer 1-10 antenna and feeding structure.

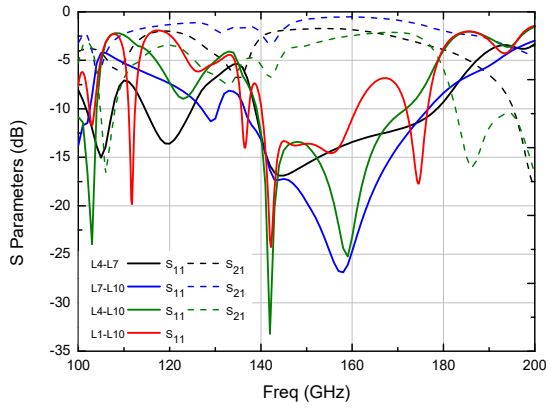

Fig. 9. Simulated reflection coefficient ($|S_{11}|$) and radiation efficiency (e_{cd}) using different feeding methods

C. 2×2 Antenna Subarray

A 4×4 subarray was simulated at 150 GHz. Only antenna element #6 from Fig. 4 was excited, and the results were compared with when the antenna element was isolated and not situated within an array. The simulated radiation patterns of the 4×4 array is shown in Fig. 10. From Fig. 11, for a 4×4 antenna array, the impedance bandwidth is 30%. Over the operating bandwidth, it can achieve 80% radiation efficiency when only antenna element #6 is excited.

D. Decoupling

For the decoupling simulation, metallic strips were added in the E-plane and H-plane between the array elements of Fig. 5. When adding the two strips in the E-plane of a 1×2 subarray as shown in Fig. 12, and in the H-plane as shown in Fig. 13, the decoupling of the array is improved.

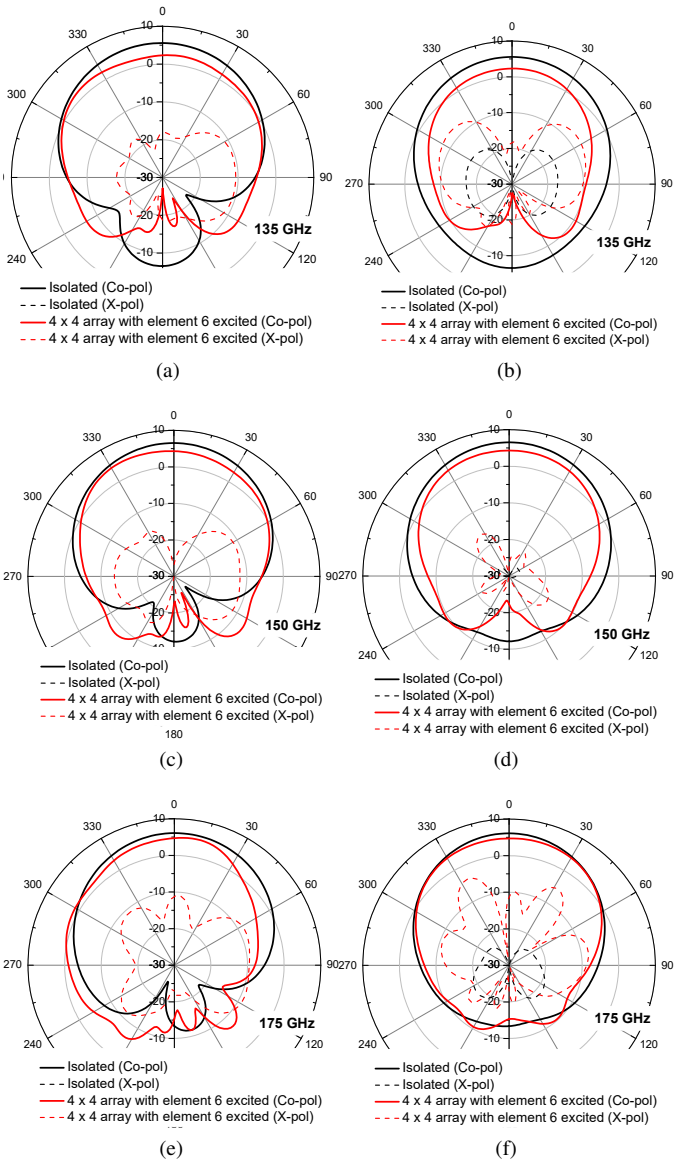

Fig. 10. Comparison of radiation patterns of isolated element and 4×4 array with element 6 excited. E-plane radiation patterns at (a) f = 135 GHz, (c) f = 150 GHz, (e) f = 175 GHz. H-plane radiation patterns at (b) f = 135 GHz, (d) f = 150 GHz, (f) f = 175 GHz

IV. Conclusion

This work proposes a multi-layered proximity-coupled probe-fed E-shaped patch antenna array for terahertz imaging system with a center frequency of 150 GHz. The E-shaped patch antenna with a meandering-probe feed using proximity coupling provides a wideband characteristic while still maintaining compatibility with fabrication limitations. A test kit was designed, fabricated, and measured to verify the design and resonance of the E-shape patch antenna using an on-wafer probe measurement setup. To connect the received antenna signal to the ICs at the bottom of the daughterboard, a feeding structure was also designed. The single E-shaped patch antenna element provides 6.02 dBi broadside realized gain, and the feeding structure contributes 3.5 dB insertion loss;

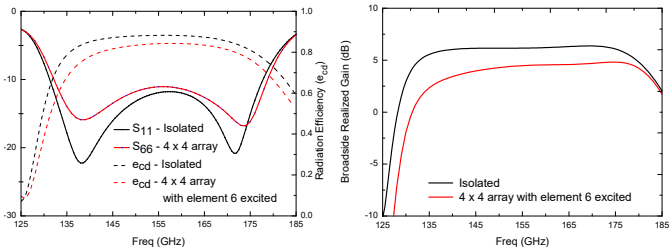

(a) a (b) b

Fig. 11. (a) Return loss (S_{11}) and radiation efficiency (e_{cd}), (b) Broadside realized gain of the E-shaped patch antenna array with element 6 excited, compared with isolated antenna element.

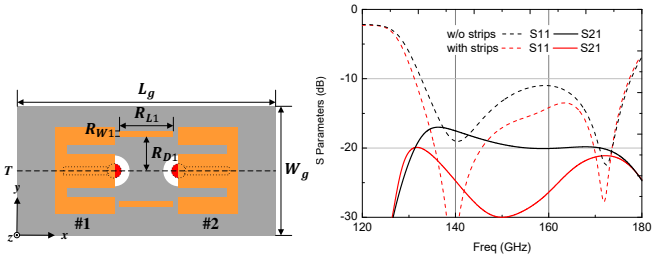

(a) (b)

Fig. 12. (a) Metallic strips added between array elements in the E-plane, (b) S-parameters of the 1×2 array with and without metallic strips added in the E-plane.

therefore the antenna and antenna feeding structure provides a 2.52 dBi gain. The E-shape patch antenna was then used to design a 4×4 subarray with an impedance bandwidth of 30% and radiation efficiency of 80% when one antenna element is excited. Metallic strips were added between the antenna elements in the E-plane and H-plane of the array to enhance decoupling between elements.

For future work, the 4×4 array with decoupling strips can be fabricated and measured to verify the proposed design in this work.

REFERENCES

[1] N. Zhu and R. W. Ziolkowski, "Photoconductive thz antenna designs with high radiation efficiency, high directivity, and high aperture efficiency," *IEEE Transactions on Terahertz Science and Technology*, vol. 3, no. 6, pp. 721–730, 2013.

[2] W. Fuscaldo, S. Tofani, D. C. Zografopoulos, P. Baccarelli, P. Burghignoli, R. Beccherelli, and A. Galli, "Systematic design of thz leaky-wave antennas based on homogenized metasurfaces," *IEEE Transactions on Antennas and Propagation*, vol. 66, no. 3, pp. 1169–1178, 2018.

[3] G. B. Wu, Y.-S. Zeng, K. F. Chan, S.-W. Qu, and C. H. Chan, "High-gain circularly polarized lens antenna for terahertz applications," *IEEE Antennas and Wireless Propagation Letters*, vol. 18, no. 5, pp. 921–925, 2019.

[4] M. S. Rabbani and H. Ghafouri-Shiraz, "Liquid crystalline polymer substrate-based thz microstrip antenna arrays for medical applications," *IEEE Antennas and Wireless Propagation Letters*, vol. 16, pp. 1533–1536, 2017.

[5] Y. Yang, O. D. Gurbuz, and G. M. Rebeiz, "An eight-element 370–410-ghz phased-array transmitter in 45-nm cmos soi with peak eirp of 8–8.5 dbm," *IEEE Transactions on Microwave Theory and Techniques*, vol. 64, no. 12, pp. 4241–4249, 2016.

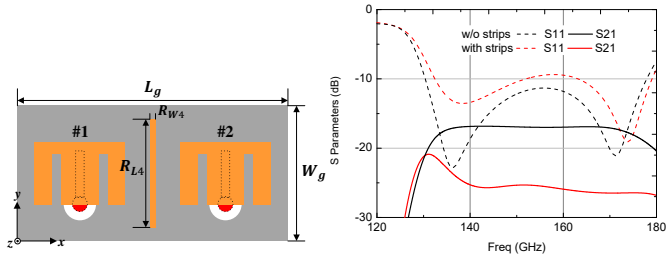

(a) (b)

Fig. 13. (a) Metallic strips added between array elements in the H-plane, (b) S-parameters of the 1×2 array with and without metallic strips added in the H-plane.

[6] Y. Tousi and E. Afshari, "A high-power and scalable 2-d phased array for terahertz cmos integrated systems," *IEEE Journal of Solid-State Circuits*, vol. 50, no. 2, pp. 597–609, 2015.

[7] F. Yang, X.-X. Zhang, X. Ye, and Y. Rahmat-Samii, "Wide-band e-shaped patch antennas for wireless communications," *IEEE Transactions on Antennas and Propagation*, vol. 49, no. 7, pp. 1094–1100, 2001.

[8] C. Mak, K. Luk, and K. Lee, "Wideband l-strip fed microstrip antenna," in *IEEE Antennas and Propagation Society International Symposium. 1999 Digest. Held in conjunction with: USNC/URSI National Radio Science Meeting (Cat. No.99CH37010)*, vol. 2, pp. 1216–1219 vol.2, 1999.

[9] C. Mak, K. Luk, K. Lee, and Y. Chow, "Experimental study of a microstrip patch antenna with an l-shaped probe," *IEEE Transactions on Antennas and Propagation*, vol. 48, no. 5, pp. 777–783, 2000.

[10] J. Xiong, Z. Ying, and S. He, "A broadband low profile patch antenna of compact size with three resonances," *IEEE Transactions on Antennas and Propagation*, vol. 57, no. 6, pp. 1838–1843, 2009.

[11] K. L. Chung and W. Y. Tam, "Particle swarm optimization of l-probe fed e-shaped patch antenna using single-objective function," *Microwave and Optical Technology Letters*, vol. 52, no. 3, pp. 702–706, 2010.

[12] W. Qiu, C. Chen, H. Zhang, and W. Chen, "A wideband dual-polarized l-probe antenna array with hollow structure and modified ground plane for isolation enhancement," *IEEE Antennas and Wireless Propagation Letters*, vol. 16, pp. 2820–2823, 2017.

[13] L. Wang, Y.-X. Guo, and W.-X. Sheng, "Wideband high-gain 60-ghz ltcc l-probe patch antenna array with a soft surface," *IEEE Transactions on Antennas and Propagation*, vol. 61, no. 4, pp. 1802–1809, 2013.

[14] K. L. Lau and K. M. Luk, "A wideband dual-polarized l-probe stacked patch antenna array," *IEEE Antennas and Wireless Propagation Letters*, vol. 6, pp. 529–532, 2007.

[15] H. Wong, K.-L. Lau, and K.-M. Luk, "Design of dual-polarized l-probe patch antenna arrays with high isolation," *IEEE Transactions on Antennas and Propagation*, vol. 52, no. 1, pp. 45–52, 2004.